Laser Desorption / Ablation Plumes from Capillary-Like Restricted Volumes

Richard Knochenmuss*
Novartis Institutes for Biomedical Research
WSJ 503.1104
4052 Basel, Switzerland

Author's final revised manuscript.
Published as Eur. J. Mass Spectrom., vol. 15, pp. 189-198 (2009)

Abstract
Laser desorption/ionization from structured surfaces has been the object of recently renewed interest. Conditions in the plume of material ablated from such surfaces may differ from those of a sample which is ablated in bulk. Since recombination and secondary ion-molecule reactions in the plume play a major role in determining the types and quantities of ions observed at the detector, these differences are analytically relevant. Desorption/ionization substrates with channels of high aspect ratio are modelled as capillary nozzles, from which free jets are emitted. A previously developed MALDI ablation/ionization model is adapted for these jets. More primary ions reach the detector when ablated from a capillary orifice, but fewer analye ions are created in secondary reactions. These differences in ion yield can persist for arrays of capillaries on the surface, depending on the ratio of their diameter to spacing.

* email: rknochenmuss@gmx.net

Introduction

The use of laser desorption/ablation substrates with sub-micrometer structure dates at least to the work of Tanaka,[1] for which he received the Nobel prize. His 60 nm Co particle substrates, and subsequent applications using carbon, silicon or other small particles,[2-8] share the feature that analytes and any matrix material are concentrated by surface tension of the preparation solution in the irregular, small gaps between the particules. Subsequent work has used porous surfaces, particulary silicon,[9-12] as well as deposits of materials with at least one sub-um dimension, such as nanowires.[13, 14] These are only examples of the wide variety of materials, preparation methods and surface morphologies that have been applied to matrix-free laser desorption/ionization.[15]

In spite of this interest, laser ablation from structured substrates has has found fewer applications than conventional MALDI. Possible reasons for this may include analyte segregation or adsorption at the substrate surface. Adhesion may be a particular problem, since thermal decomposition becomes more probable than desorption as the molecular weight increases.[16, 17] Nevertheless, the methods are effective for some otherwise intractable analytes, such as terpenoid resins,[18] or small metabolites,[19] and could be considered more often for difficult samples of modest molecular weight. The method may also have untapped potential, since enhanced sensitivity has recently been demonstrated for ablation of thin samples on some metals, due to electronic interactions with matrix molecules.[20, 21] Optimized combinations of surface material, matrix and surface structure could result in useful methods for many applications

Among the more promising of recent such approaches are substrates with deep pores. The high aspect ratio seems to be an important contributor to the efficacy, although the reasons for this are not yet clear. It may be a combination of factors including efficient laser absorption, low thermal conductivity of rod tips to the bulk, entrapment of sample in the pores, or modification of the ablation plume characteristics. Only the latter aspect is investigated here, all factors influencing the primary ion yield will be excluded.

The ablation plume has a large effect on MALDI analytical efficiency, since it is where reactions with primary matrix ions lead to most analyte ions.[22, 23] A similar two step model should be applicable to substrate ablation techniques which use a matrix. Matrix may be intentionally added, or be a result of the substrate and preparation method, such as when water or other solvent is retained in pores or between particles or wires. Capillary-like structures are predicted to create a faster, more directed plume, which is favorable for primary ion release. Secondary ion formation in the plume is, however, less extensive than in bulk ablation.

Theory and Model

A rate equation model for conventional MALDI has been reported.[24, 25] An important aspect of the model is the coupling of the plume expansion with the ion chemistry. After the laser pulse generates ions, the expansion prevents the system from relaxing fully back to a state with no free charge. This expansion-dependent net ion yield is the analytically useful output of the method.

In the model of refs. 24, 25 the plume expansion was treated as a free jet emanating from an "orifice" corresponding to the laser spot. The classical free jet description was modified slightly to account for the acceleration of the ablated material by thermal expansion prior to phase change, as also seen in molecular dynamics simulations of laser ablation and

MALDI.[26] This picture is supported by and reproduces the observed dependence of MALDI ion yield on laser spot diameter.[27]

It has long been known in the molecular beam community that nozzle geometry has a significant effect on jet characteristics.[28] The manner in which isotropically oriented thermal motion is converted to directed mass flow depends on the transition region defined by the nozzle, because it establishes the streamlines that are propagated into the low pressure region. In addition to the net stream velocity attained, these also determine the collision and diffusion rates at all points downstream. These are the quantities which modulate the rate of ion recombination and secondary ion-molecule reactions in an ablation plume.

Recent structured substrates are characterized by deep pores of high aspect ratio. For the material ejected out of these the pores, the environment may approximate a long capillary. Murphy and Miller have calculated the characteristics of a gas expansion from a capillary nozzle and compared it directly to that of an ideal nozzle of negligible thickness.[29] From their Fig. 4 it is apparent that a capillary nozzle results in higher centerline Mach numbers, meaning that the gas is more strongly accelerated along the expansion axis. From the Mach number all other gas parameters in the ablation plume can be calculated.

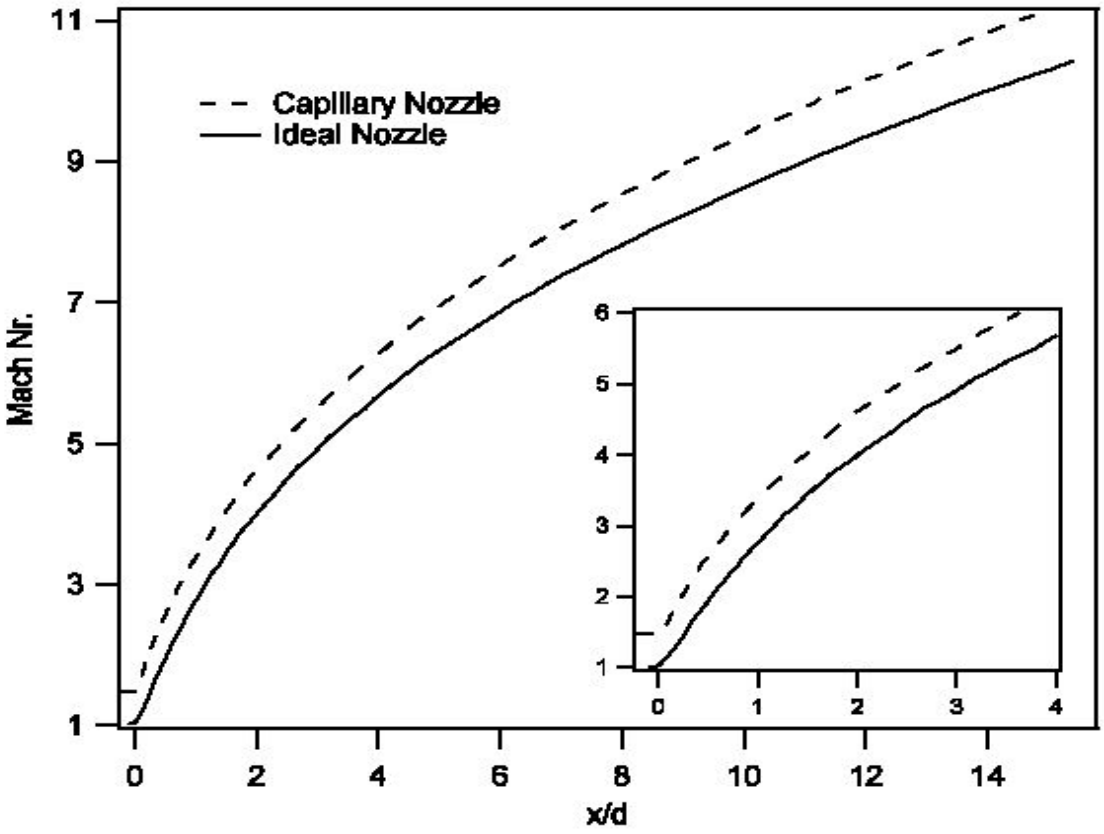

Figure 1. Axial Mach number vs. downstream distance for ideal and capillary nozzles, as reported in Ref. 29. The horizontal axis uses the dimensionless characteristic ratio of distance, x, over the nozzle diameter, d.

Ablation from a planar MALDI sample surface comes close the the ideal of negligible nozzle thickness. In the case of UV ablation, the ablation depth is 10s to 100s of nm, while the spot size is micrometers, and usually much more. There is essentially no radial confinement prior during ejection. In IR ablation, the ablation depth is considerably larger, corresponding to the

lower absorption cross section.[27] It is still only a few microns, which is very thin by comparison to conventional molecular beam nozzles. Nevertheless, to avoid implying that the non-capillary MALDI geometry is in some sense optimum, it will be referred to below as the flat planar surface, or FPS.

The calculations of Murphy and Miller considered a geometry that resulted in gas acceleration to about Mach 1.5 before reaching the capillary exit. Because the surface pores are much shorter than a macroscopic capillary this degree of initial acceleration is not expected in the present case. However, the acceleration due to rapid thermal expansion prior to phase change remains. Based on these considerations, the capillary modification to the existing MALDI model is taken to be the excess capillary Mach number vs. the FPS case of Fig. 1, after subtraction of the initial acceleration of the macroscopic nozzle.

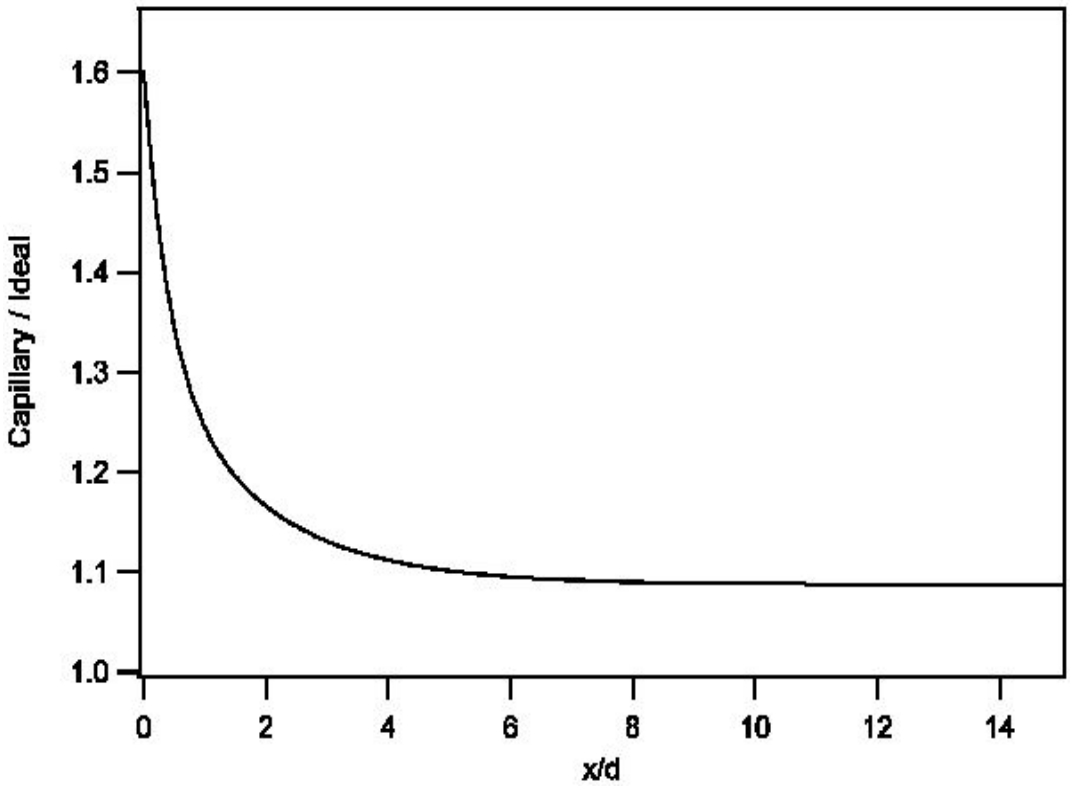

Figure 2. Ratio of capillary to FPS Mach number as used to model the plume characteristics in the MALDI ionization and ablation model.

The factor multiplying the FPS Mach number is shown in Fig. 2. This was fit to a 4th order polynomial and used to modify the plume expansion characteristics of the model. All second order processes are influenced by the collision rate calculated from this, including ion recombination, and secondary charge transfer reactions between ions and neutrals. The latter includes reaction of primary ions to create secondary analyte ions, as well as analyte-analyte charge exchange reactions.

Bulk vs. Surface or Capillary Ablation

The model was initially developed for ultraviolet laser ionization in bulk matrix. It is also applicable to capillaries because it includes no explicit lateral dimension. The plume pressure drops due to both axial and radial expansion, but the radial part is implicit in the dependence of intensive quantities on downstream displacement. This arises from the isentropic nature of

the expansion, and allows the volume modeled to be considered either an isolated bulk piece of material (the original application), or the ablated volume adjacent to a capillary wall (if the wall length is short compared to the overal expansion distance, which is the case in these applications and in molecular beams).

On a capillary surface, the primary ion yield may be different than in a bulk matrix, and the ions may be formed by a different mechanism.[30, 31] However, the initial absolute yield is not of interest here, but rather the influence of plume expansion properties on the evolution of the initial ions. A different initial ion quantity does not change the relative properties of free and capillary plumes, only the overall ion yield for both.

The same holds for radial ion concentration gradients in the capillary. These might arise due to analyte surface adsorption, or different primary ionization mechanisms and yields on the wall vs. in the bulk. Radial diffusion would change the ion concentrations in the modelled volume over time, but in the absence of extremely large differences in recombination rates (which are not predicted) this represents a scale factor which cancels when comparing free and capillary plumes.

Thanks to the implicit radial dependence of the model, the plume comparisons are considered valid for ions formed by any mechanism in the capillary pores, although the primary ionization of the original model is retained. Not included in this model are the effects of temperature and pressure gradients in the capillary if the laser is absorbed predominantly on the capillary walls. This will be most relevant during the stress confinement period investigated by molecular dynamics simulations of MALDI with short pulse irradiation.[32-35] Since this is expected only the first nanoseconds of the process, its effects will be minimal for the vast majority of the expansion which is if interest here.

Results and Discussion

Primary Ion Survival

The laser pulse energy (and to a lesser extent by the pulse width) largely determines how much material is ablated, the temperature of the plume, and the charge density at the time of phase change. After the phase change, recombination reduces the ion yield significantly, as seen in the example results of Fig. 3. The plume modulates recombination via time-dependent pressure, temperature and density.

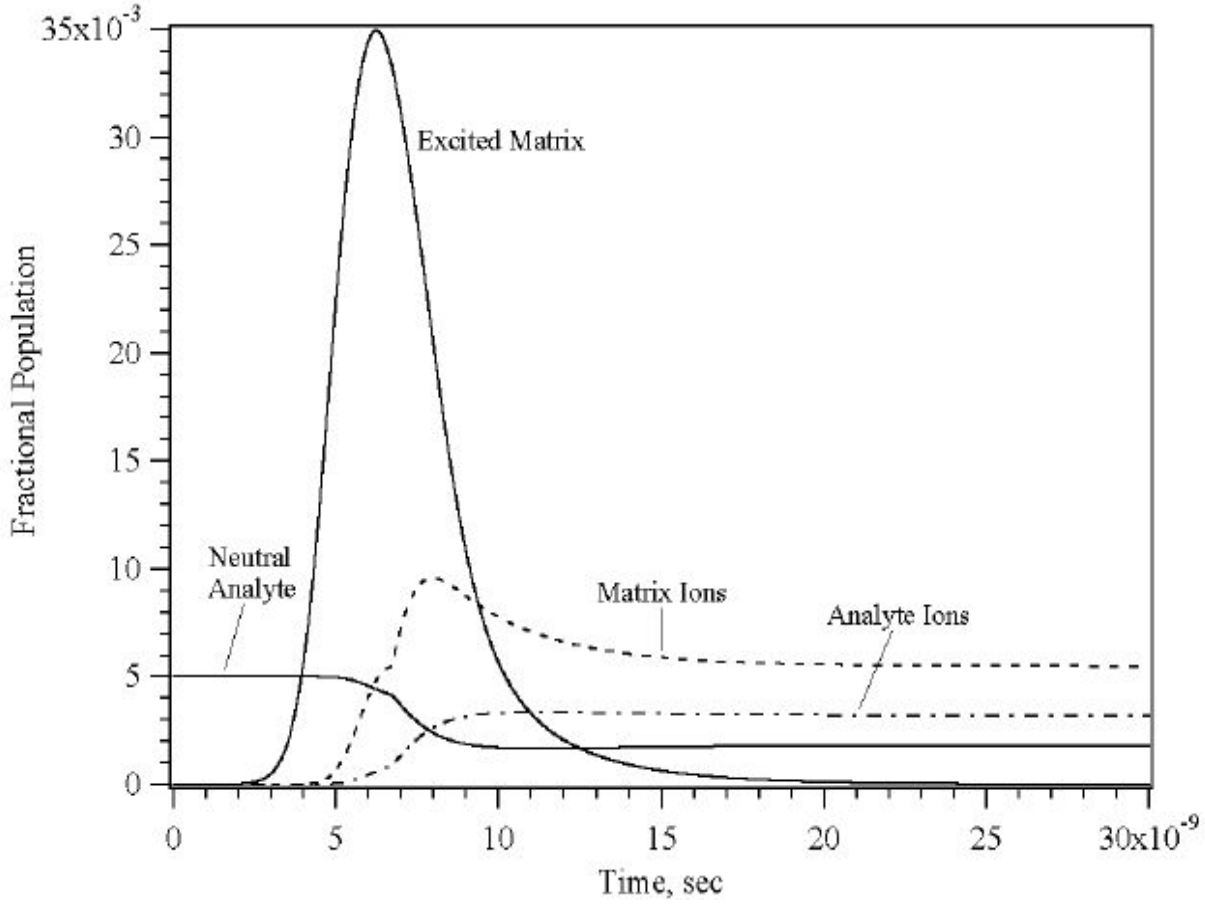

Figure 3. Fractional populations of some key species during a MALDI event, calculated using the rate equation model of Refs. 24, 25: The laser pulse was a 5 ns fullwidth, 20 mJ/cm2, 355 nm Gaussian, centered at 6 ns. The phase change took place near 7 ns, at a temperature of 450 K. After the phase change, the rates of all intermolecular processes are determined by the plume expansion characteristics.

As seen in Fig. 4, the capillary expansion model predicts a higher net primary ion yield at all fluences above the threshold for ablation, because of faster expansion to regimes of lower collision rate. The increase in yield is modest, and slightly larger at higher fluences, not exceeding about 1/3 of the non-capillary yield.

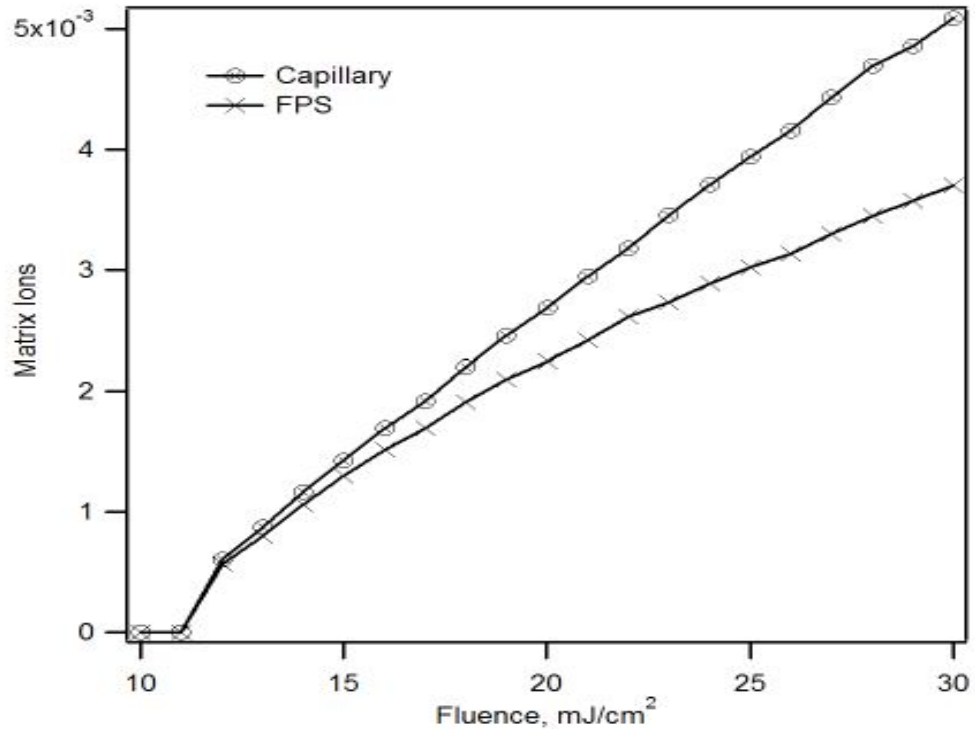

Figure 4. Fractional matrix ion yield as a function of laser fluence, for a 5 ns, 355 nm pulse. The faster capillary expansion allows more ions to reach the detector.

From this result it appears that a pure LDI experiment, in which only the analyte is present on the structured surface, would benefit from a modestly improved ion yield vs. a less structured surface. In addition the structured surface may carry a substantially higher analyte load, due to its surface area. However, such a simple experiment is probably rarely realized in practice. Either matrix is intentionally added, as when using thin MALDI samples or surfactants,[36] or the structured surface retains water or solvent from the preparation solution. In addition, an ablatable surface layer may exist due to the structuring technique.[37] Hence it is also important to consider the case of analyte in an ionizable environment.

Secondary Ion Formation

The ionizable environment will be denoted "matrix" for brevity, but need not be a classical MALDI matrix substance. This matrix may take at least two forms. Either the matrix functions in the conventional MALDI manner as a photoionizable absorber of the incident energy, or it is ionized at the capillary wall, either directly or in an indirect charge transfer process. In either case, the typical excess of matrix (e.g. solvent) makes it more likely that analyte molecules will encounter a primary ion in the plume than that they will be directly ionized (a disparity which increases with the size of the analyte). If this is not true, for example because the analyte is only ionized in contact with the capillary walls, the experiment is essentially LDI, not MALDI, and the results of Fig. 3 largely apply.

To examine the ionizable matrix case, analytes are taken to be entirely ionized by reaction with primary ions. The rate of analyte ionization, and subsequent survival yield, are highly dependent on collision rates in the plume. The capillary plume was found above to be advantageous for the survival of primary ions, but it also means that collisions leading to secondary charge transfer reactions are fewer. The net result of these counteracting effects is seen in Fig. 5.

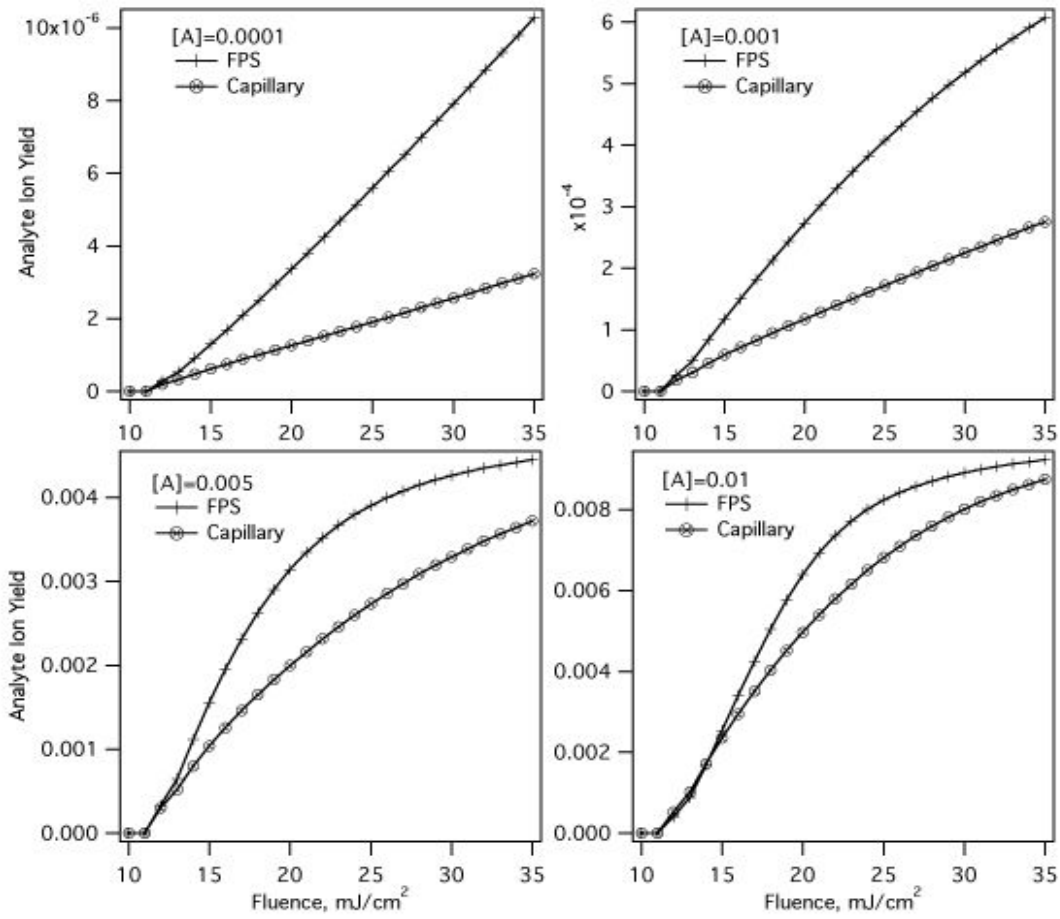

Figure 5. Capillary and FPS analyte fractional ion yields for different initial analyte concentrations (mole fraction), as a function of laser fluence.

At lower analyte concentrations, the secondary ion yield is determined most by the probability of collision with primary ions. Since this decreases rapidly in the capillary expansion, the analyte signal is significantly reduced vs. the FPS expansion. More concentrated analyte has a higher probability of reacting early with primary ions, before the plume becomes dilute. In this case analyte yield is influenced mostly by recombination losses, which are similar for primary and secondary ions.

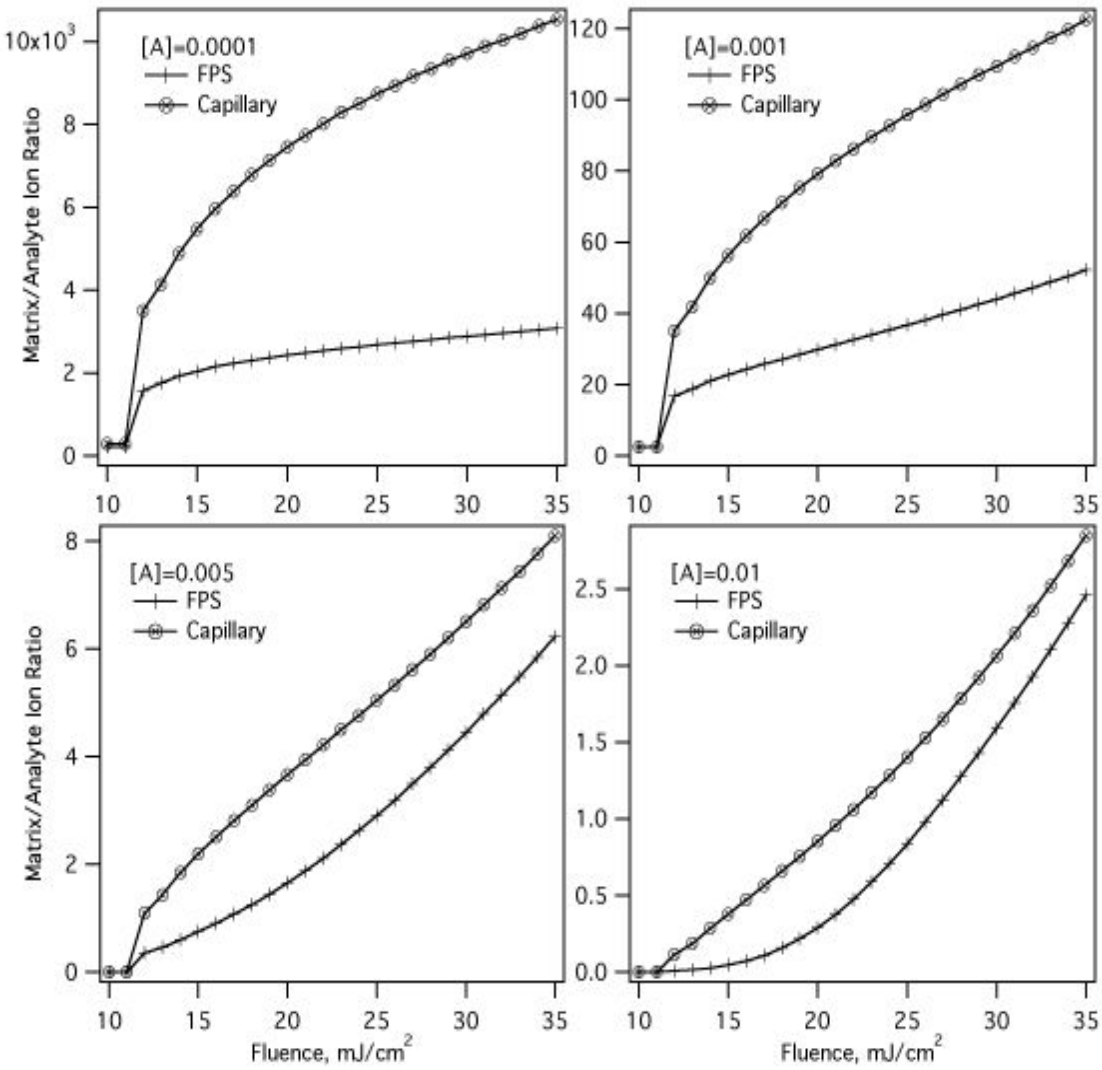

Figure 6. Matrix/analyte ion ratios for different initial analyte concentrations (mole fraction), as a function of laser fluence.

Also important for spectral quality and detection of smaller analytes is the ratio of primary to secondary ion yields. A high ratio is undesirable, since small analyte signals can be lost in the background of matrix-related ions. As seen in Fig. 6, this ratio is distinctly worse for the capillary plume, although it improves at higher analyte concentration. The ratio is always best at lowest fluence, since the excess of primary ions is lower. This comes at the cost of lower sensitivity, since the absolute primary and secondary yield is then lower as well.

Arrays of Capillaries

The above results suggest that an isolated capillary-like ion source would be disadvantageous under many circumstances, even without taking into consideration possible other losses, such as surface adhesion of analyte. (In the sense that it is not ablatable. If surface adsorption increases direct analyte ionization, this is obviously favorable, so long as the ions are also subsequently ablated.) However, real surfaces are comprised of many such emitters, of variable dimension and spacing. If the microscopic plumes merge near the surface, the overall macroscopic plume characteristics would be equivalent to a conventional, FPS plume. It is therefore important to understand the conditions under which this could be the case.

Fig. 7 shows plume velocities calculated for FPS and capillary plumes. After the phase change they both are in the range of 500 m/s, corresponding to 0.5 um/ns. As seen in Fig. 3, there is a transition period of about 10 ns after vaporization during which primary ion formation and secondary charge transfer peak and are overtaken by recombination. As the plume accelerates and expands, recombination losses slow dramatically so the yield is determined most by the plume properties in the transition period. This period represents an expansion distance of about 5 um.

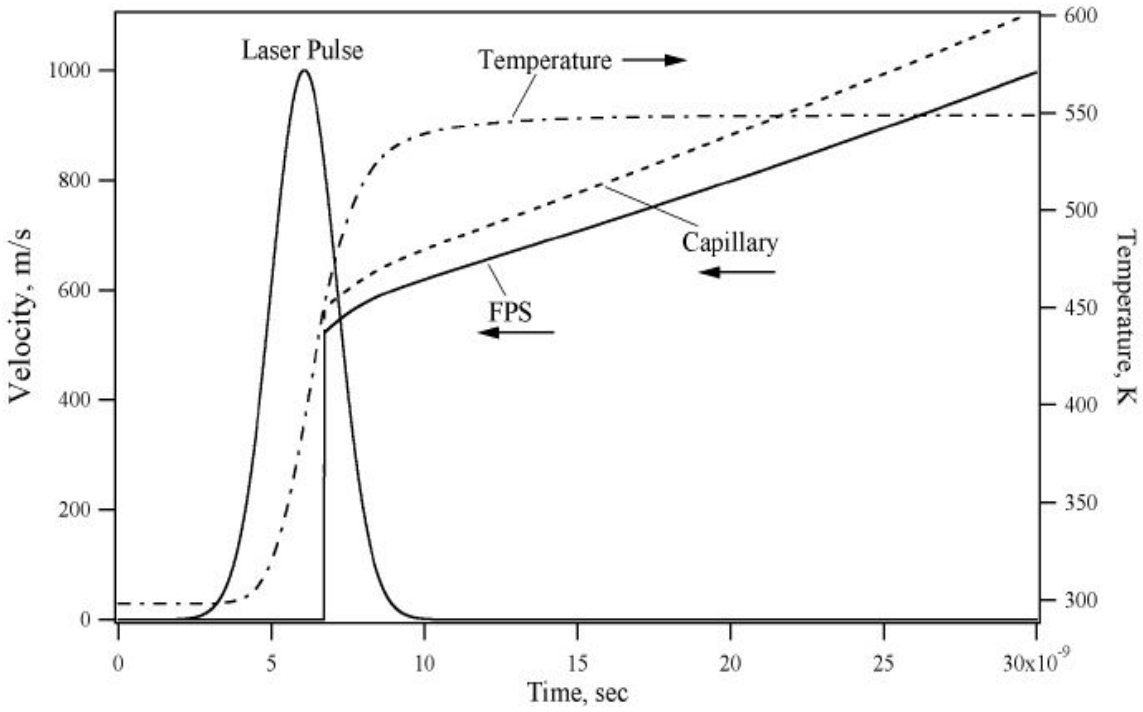

Figure 7. FPS and capillary plume velocities vs. time, as calculated for conditions similar to Fig. 3.

The lateral expansion of the plume from a single small capillary can be estimated from the properties of macroscopic FPS expansions. As seen Fig. 8, a FPS free jet expands in a roughly conical manner at distances of a few nozzle diameters. About 8 diameters of axial expansion are required for the gas to reach 50 % density at a lateral distance of 5 diameters. At this density, neighboring plumes would merge significantly. Because of its more directed nature, a capillary plume has a slower lateral expansion, so this represents a lower limit for plume interaction distances and times.

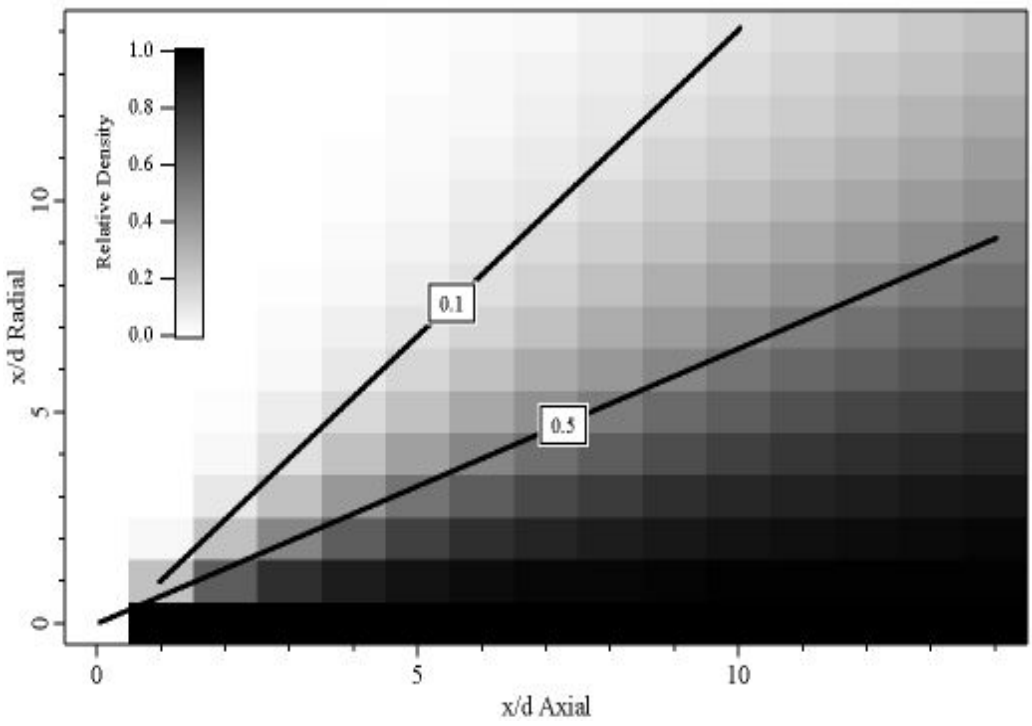

Figure 8. Density of a FPS free jet expansion as a function of axial and radial distance from the orifice, from Refs.38,28. The approximate 10 and 50 percent density boundaries are indicated by the labeled lines.

Plume merging then depends on the ratio of the effective orifice to the distance between orifices. The interplay between these factors is illustrated in Fig. 9. Very small channels, with close spacing, merge quickly. However, already at a diameter of 3 um, a very tight spacing of only 1 diameter has a relatively long merge time of 10 ns. Note again that this is for FPS plumes, tighter capillary plumes will merge slower. Merge times of 10 ns or more are long enough that the conclusions above regarding isolated capillaries largely apply.

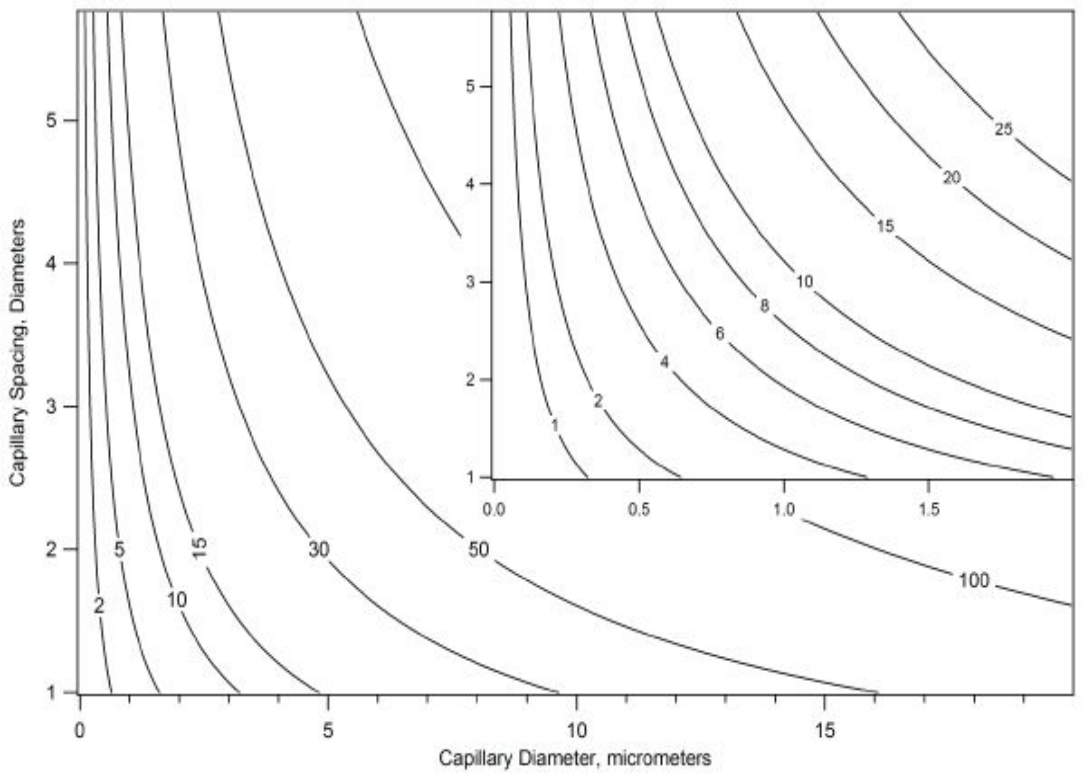

Fig 9. Contour plot of the time after start of ablation to merging of adjacent expanding FPS plumes, in nanoseconds. A merge is defined as meeting of the 50 % density radii, as the plume expands downstream. The inset shows an expansion of the small diameter region.

Conclusions

The properties of laser desorption plumes generated from capillary-like pores, orifices or channels are predicted to be significantly different from those of plumes arising from a closed, plane surface. The capillary plume reaches higher Mach numbers faster, resulting in fewer collisions. More primary ions are thereby released from the plume, making the structured surface preferable for applications where the analyte can be ionized and desorbed without assistance from an ionizable matrix (either surface or bulk).

If secondary ion-molecule reactions are involved in analyte ion generation, the faster capillary expansion is disadvantageous. In spite of an increased primary ion yield, charge transfer reactions are less efficient than in the FPS plume, so net analyte yield is lower. This is particularly true at medium to low analyte concentrations in the sample.

The ion yield of an array of capillary emitters may be more like an isolated capillary plume or a FPS plume, depending on the ratio of orifice spacing to orifice diameter. Very small diameter emitters (sub-micrometer) will exhibit FPS plume characteristics, even when closely spaced. Up to about 3 micrometers diameter, the spacing may be close enough to reach FPS behavior in the time period necessary for most ion-molecule reactions. Above this size, even spacing of 1 diameter is insufficient for early coalescence, and the ion distribution will be like that of a capillary expansion.

References

1. K. Tanaka, H. Waki, Y. Ido, S. Akita, Y. Yoshida, T. Yoshida, "Protein and Polymer Analyses of up to m/z 100,000 by Laser Ionization Time-of-Flight Mass Spectrometry", *Rapid Commun. Mass Spectrom.* **2**, 151 (1988).
2. J. Sunner, E. Dratz, Y. Chen, "Graphite Surface-Assisted Laser Desorption/Ionization Time-of-flight Mass Spectrometry of Peptides and Proteins from Liquid Solutions", *Anal. Chem.* **67**, 4335 (1995).
3. M. Han, J. Sunner, "An activated carbon substrate surface for laser desorption mass spectrometry", *J. Am. Soc. Mass Spectrom.* **11**, 644 (2000).
4. M. J. Dale, R. Knochenmuss, R. Zenobi, "Graphite/Liquid Mixed Matrices for Laser Desorption/Ionization Mass Spectrometry", *Anal. Chem.* **68**, 3321 (1996).
5. M. J. Dale, R. Knochenmuss, R. Zenobi, "Two-Phase MALDI - Matrix Selection and Sample Pretreatment for Complex Anionic Analytes", *Rapid Commun. Mass Spectrom.* **11**, 136 (1997).
6. M. Schüenberg, Physik Westfälische Wilhelms-Universität Münster, Münster (1996).
7. M. Schürenberg, K. Dreisewerd, F. Hillenkamp, "Laser desorption/ionization mass spectrometry of peptides and proteins with particle suspension matrices", *Anal. Chem.* **71**, 221 (1999).
8. J. A. McLean, K. A. Stumpo, D. H. Russell, "Size selected (2-10 nm) gold nanoparticles for matrix assisted laser desorption of peptides", *J. Am. Chem. Soc.* **127**, 5304 (2005).
9. J. Wei, J. M. Burlak, G. Siuzdak, "Desorption-ionization mass spectrometry on porous silicon", *Nature* **399**, 243 (1999).
10. Y. Chen, A. Vertes, "Adjustable Fragmentation in Laser Desorption/Ionization from Laser-Induced Silicon Microcolumn Arrays", *Anal. Chem.* **78**, 5835 (2006).
11. Q. Zhang, H. Zou, Z. Guo, B. C. Guo, "Matrix Assisted Laser Desorption/Ionization Mass Spectrometry using Porous Silicon and Silica Gel as a Matrix", *Rapid Comm. Mass Spectrom.* **15**, 217 (2001).
12. R. Nayak, D. R. Knapp, "Effects of Thin-Film Structural Parameters on Laser Desorption/Ionization from Porous Alumina", *Anal. Chem.* **79**, 4950 (2007).
13. S. Y. Xu, Y. F. Li, H. F. Zou, J. S. Qiu, Z. Guo, B. C. Guo, "Carbon nanotubes as assisted matrix for laser desorption/ionization mass spectrometry", *Anal. Chem.* **75**, 6191 (2003).
14. G. E.P., J. V. Apon, G. Luo, A. Saghatellan, R. H. Daniels, V. Sahl, R. Dubrow, B. F. Cravatt, A. Vertes, G. Siuzdak, "Desorption/Ionization on Silicon Nanowires", *Anal. Chem.* **77**, 1641 (2005).
15. D. S. Peterson, "Matrix-free methods for laser desorption/ionization mass spectrometry", *Mass Spect. Rev.* **26**, 19 (2007).
16. M. Handschuh, S. Nettesheim, R. Zenobi, "Is Laser-Heating Advantageous for Thermal-Desorption of Large Polar-Molecules?", *J. Chem. Phys.* **107**, 2603 (1997).
17. M. Handschuh, S. Nettesheim, R. Zenobi, "Laser-Induced Molecular Desorption and Particle Ejection from Organic Films", *Appl. Surf. Sci.* **137**, 125 (1998).
18. P. Dietemann, K. M., S. Zumbühl, R. Knochenmuss, S. Wülfert, R. Zenobi, "A mass spectrometry and electron paramagnetic resonance study of photochemical and thermal aging in triterpene varnishes", *Anal. Chem.* **72**, 2087 (2001).
19. H. Zhang, S. Cha, E. S. Yeung, "Colloidal Graphite-Assisted Laser Desorption/Ionization MS and MSn of Small Molecules. 2. Direct Profiling and MS Imaging of Small Metabolites from Fruits", *Anal. Chem.* **79**, 6575 (2007).
20. R. Knochenmuss, G. McCombie, M. Faderl, "The dependence of MALDI ion yield on metal substrates: photoelectrons from the metal vs. surface-enhanced matrix photoionization", *J. Phys. Chem. A* **110**, 12728 (2006).
21. G. McCombie, R. Knochenmuss, "Enhanced MALDI ionization efficiency at the metal-matrix interface: practical and mechanistic consequences of sample thickness and preparation method", *J.Am. Soc. Mass Spectrom.* **17**, 737 (2006).
22. R. Knochenmuss, "Ion formation mechanisms in UV-MALDI", *The Analyst* **131**, 966 (2006).
23. R. Knochenmuss, A. Stortelder, K. Breuker, R. Zenobi, "Secondary ion-molecule reactions in MALDI.", *J. Mass Spectrom.* **35**, 1237 (2000).
24. R. Knochenmuss, "A Quantitative Model of Ultraviolet Matrix-assisted Laser

Desorption and Ionization", *J. Mass Spectrom.* **37**, 867 (2002).
25. R. Knochenmuss, "A Quantitative Model of UV-MALDI Including Analyte Ion Generation", *Anal. Chem.* **75**, 2199 (2003).
26. R. Knochenmuss, L. V. Zhigilei, "A molecular dynamics model of UV-MALDI including ionization processes", *J. Phys. Chem. B* **109**, 22947 (2005).
27. K. Dreisewerd, M. Schürenberg, M. Karas, F. Hillenkamp, "Influence of the Laser Intensity and Spot Size on the Desorption of Molecules and Ions in Matrix-Assisted Laser-Desorption/Ionization with a Uniform Beam Profile", *Int. J. Mass Spectrom. Ion Proc.* **141**, 127 (1995).
28. D. R. Miller, "Free Jet Sources", **Atomic and Molecular Beam Methods 1**, 14 (1988).
29. H. R. Murphy, D. R. Miller, "Effects of Nozzle Geometry on Kinetics in Free-Jet Expansions", *J. Phys. Chem.* **88**, 4474 (1984).
30. G. Luo, Y. Chen, H. Daniels, R. Dubrow, A. Vertes, "Internal Energy Transfer in Laser Desprotion/Ionization from Silicon Nanowires", *J. Phys. Chem. B* **110**, 13381 (2006).
31. Y. Chen, H. Chen, A. Aleksandrov, T. M. Orlando, "Roles of Water, Acidity and Surface Morphology in Surface-Assisted Laser Desorption/Ionization of Amino Acids", *J. Phys. Chem. C* **112**, 6953 (2008).
32. L. V. Zhigilei, B. J. Garrison, "Microscopic mechanism of laser ablation of organic solids in the thermal stress confinement irradiation regime", *J. Appl. Phys.* **88**, 1 (2000).
33. L. V. Zhigilei, P. B. S. Kodali, B. J. Garrison, "A Microscopic View of Laser Ablation", *J. Phys. Chem. B* **102**, 2845 (1998).
34. L. V. Zhigilei, E. Leveugle, B. J. Garrison, Y. G. Yingling, M. I. Zeifman, "Computer Simulations of Laser Ablation of Molecular Substrates", *Chem. Rev.* **103**, 321 (2003).
35. L. V. Zhigilei, Y. G. Yingling, T. E. Itina, T. A. Schoolcraft, B. J. Garrison, "Molecular dynamics simulation soft matrix-assisted laser desorption- connections to experiment", *Int. J. Mass Spectrom.* **226**, 85 (2003).
36. T. R. Northen, O. Yanes, N. M.T., D. Marrinucci, W. Uritboonthai, J. Apon, S. Golledge, A. Nordström, G. Siuzdak, "Clathrate nanostructures for mass spectrometry", *Nature* **449**, 1033 (2007).
37. T. R. Northen, H.-K. Woo, M. Northen, A. Nordström, W. Uritboonthail, K. L. Turner, G. Siuzdak, "High Surface Area of Porous Silicon Drives Desorption of Intact Molecules", *J.Am. Soc. Mass Spectrom.* **18**, 1945 (2007).
38. J. B. Anderson, "Off axis molecular beam properties", *AIAA J.* **10**, 112 (1972).